SAND2011-0748C

7^{th} US National Technical Meeting
of the Combustion Institute
Hosted by the Georgia Institute of Technology, Atlanta, GA
March 20–23, 2011

A Computational Study of Pulsating Instabilities in Externally Forced 1D and 2D Premixed Flames

Gaurav Bansal and Jacqueline H. Chen

Reacting Flow Research Department, Combustion Research Facility, Sandia National Laboratories, Livermore, CA - 94551

In this study, the pulsating instability mode in near-rich limit strained hydrogen/air premixed flames is investigated using high-fidelity numerical techniques by incorporating detailed chemical kinetics. For these flames, the Lewis number of the deficient reactant is sufficiently greater than unity and the Zeldovich number is large. This pulsating mode becomes practically relevant in determining the flammability limits of such flames as the definition based on steady flammability limit becomes inadequate. The effects of an external forcing, in the form of an imposed strain rate fluctuation in time, on these intrinsic pulsating instabilities are also examined in a counterflow configuration. A range of frequencies of this imposed strain rate fluctuation is investigated. These effects become important when the flame propagates in an unsteady flow field, for example, in turbulent flows. Based on the insights gained from 1D simulations, 2D simulations of these pulsating flames are performed next, in a reactant-to-product (RtP) counterflow configuration. 2D simulations provide additional insights on the shape and location of cells and cusp formation in these flames due to the coupled effects of pulsating and hydrodynamic instabilties.

1 Introduction

It is well known, through a variety of theoretical [1, 2], computational [3, 4], and experimental [5] studies, that if the Lewis number of a combustible mixture sufficiently exceeds unity, the propagation of a planar premixed flame could demonstrate a pulsating mode, especially for near-limit weakly burning flames. The existence of such a pulsating mode becomes important in estimation of flammability limits of premixed flames since by definition flammability limit is a limit phenomenon. As such, it has been shown in previous studies [2, 6] that the presence of a pulsating instability mode may lead to a narrower flammability range when compared to that predicted by assuming steady flame propagation. The pulsating instability analysis by Sivashinsky [1], with one-step chemistry, constant property assumptions, yielded a criterion for the onset of oscillation:

$$\mathrm{Ze}(\mathrm{Le}-1) > 4(1+\sqrt{3}) \approx 11 \tag{1}$$

where

$$\mathrm{Ze} = \frac{E_a(T_b^0 - T_u)}{R(T_b^0)^2} \tag{2}$$

is the Zeldovich number, E_a is the effective activation energy, R is the universal gas constant, T_b^0 is the adiabatic flame temperature, and T_u is the unburned gas temperature. For sufficiently rich hydrogen/air flames, the Lewis number is greater than one, and one can satisfy this inequality by increasing equivalence ratio (ϕ), thus increasing E_a and decreasing T_b^0, both of which increase Ze. Moreover, the other two parameters that can significantly affect this inequality are the pressure (p)

and strain rate (κ). The role of pressure can be elucidated by considering detailed chemical kinetics as is also demonstrated in Ref. [3]. Essentially, for hydrogen/air flames, a change in pressure can influence the relative efficiencies of the two-body reaction, R1, and the three-body reaction, R9:

$$\mathrm{H} + \mathrm{O_2} \rightarrow \mathrm{O} + \mathrm{OH} \tag{R1}$$

$$\mathrm{H} + \mathrm{O_2} + \mathrm{M} \rightarrow \mathrm{HO_2} + \mathrm{M} \tag{R9}$$

This alters the effective activation energy of the system as the pressure is varied. A stability map for hydrogen/air flames in p and ϕ coordinates is given in Figure 18 of Ref. [3]. Effects of strain rate (κ) were studied in Refs. [2, 6]. It is known that for Le > 1 flames, positive strain weakens the flame, thus increasing E_a and reducing T_b^0, and therefore, promoting pulsation.

In the present study, we computationally investigate the pulsating instability phenomenon in near rich-limit hydrogen/air counterflow premixed flames with detailed chemical kinetics at elevated pressures. In light of the existing literature, the specific objective of the present study is to understand the behavior of pulsating flames in unsteady flow fields. In particular, we aim to study the interaction between intrinsic flame pulsating instability with an externally imposed forcing, which in the present study takes the form of an imposed fluctuation in strain rate. Both one- and two-dimensional simulations are conducted. For the one-dimensional flame, a symmetric twin flame configuration is adopted, and an extensive parametric study is conducted by varying the frequency of the imposed strain rate fluctuation. Two-dimensional simulations are subsequently conducted by adopting a reactant-to-product (RtP) configuration, and provide additional insights into the shape and location of cells and cusp formation on the flame surface due to the coupled effects of pulsating and hydrodynamic instabilities.

2 Numerical Methodology

For the one-dimensional (1D) results, presented in Section 3, the model configuration is a symmetric counterflow, which results in twin premixed flames. Only half of the domain is actually solved because of symmetry. For this configuration, the unsteady one-dimensional conservation equations for mass, momentum, and energy, in cylindrical coordinates, are derived along the centerline in a one-dimensional form. Details of formulation and numerical algorithm can be found in Ref. [7]. The code is interfaced with CHEMKIN [8] and Transport [9] libraries for computing detailed reaction rates, and thermodynamic and transport properties. Adiabatic boundary conditions are employed at the stagnation plane boundary. To impose unsteady strain rate on the flames, an unsteady velocity boundary condition of the form given in Eq. 3 is imposed at the nozzle inlet.

$$\mathrm{V_{inlet}}(t) = \mathrm{V_0}\left(1 + A\left(1 - \cos\left(2\pi f t\right)\right)\right) \tag{3}$$

where A and f correspond to the amplitude and frequency of the imposed sinusoidal velocity oscillation, respectively. $\mathrm{V_0}$ is the initial velocity at time, $t = 0\ ms$. To conduct unsteady simulations, a steady solution profile is first obtained for the nozzle inlet velocity of $\mathrm{V_0}$, and then the unsteady simulation is performed with the steady result as the initial solution.

The size of the domain is fixed to 2.5 mm for all cases (x = 0 is the left stagnation plane boundary, and x = 2.5 mm is the right nozzle inlet boundary). A uniform mesh with 300 grid points is used. This gives a spatial resolution of 8.34 μm. The consumption speed for hydrogen flame is defined as in Ref. [10]:

$$\mathrm{S_{cons}} = \frac{\int \omega_k d\mathrm{x}}{\rho_u \left(Y_{k,b} - Y_{k,u}\right)} \tag{4}$$

where ω is the reaction rate, ρ_u is the upstream density, Y is the mass fraction, subscripts u and b denote the unburned and burned sides, respectively, and k corresponds to hydrogen specie.

For the two-dimensional (2D) results, presented in Section 4, a reactant-to-product (RtP) counterflow configuration is adopted. The full compressible Navier-Stokes, species, and energy equations for a reacting gas mixture, in axisymmetric cylindrical coordinates, are solved using a fourth-order Runge-Kutta method for time integration and an eight-order explicit spatial difference scheme [11, 12]. Non-reflecting outflow boundary condition [13] is applied on the top boundary, and soft inflow boundary condition is applied on left and right boundaries. Symmetry conditions are specified at the polar axis (bottom boundary). Plug flow boundary conditions are specified at inlets. For further details on computational methodology and boundary conditions the reader is referred to Ref. [14]. Reactants enter from the right boundary (axial location, x = 5 mm), and adiabatic products enter from the left boundary (axial location, x = 0 mm). The domain length in the radial direction is 5 mm. A uniform mesh with 600 grid points in the axial direction, and 400 grid points in the radial direction is used. This gives a spatial resolution of 8.34 μm in the axial direction (same as 1D simulation), and 12.5 μm in the radial direction.

For both 1D and 2D simulations, a detailed hydrogen/air chemical mechanism [15], and mixture-averaged transport properties are used. Also for both 1D and 2D simulations, the thermodynamic pressure of the system is fixed at 20 atm, the inlet temperature of the fuel/air mixture is fixed at 298 K, and hydrogen/air equivalence ratio is fixed to 5.0, for all the cases studied. The pressure and equivalence ratio conditions were chosen such that the pulsating instability mode appears (based on guidance from Figure 18 of Ref. [3]).

3 One-Dimensional Flame Results

In this section, we present results from the 1D simulations. Figure 1 shows the upper-branch of the inverse S-curve for this flame, where the steady state value of maximum temperature in the domain is plotted against the flow inlet velocity (V_{inlet}). From this figure, the extinction turning point is found to occur at V_{inlet} = 30 cm/s. To investigate the pulsating instability mode, we start from a steady state solution as the initial conditions, and evolve the solution in time, with all boundary conditions fixed to the steady state computation. It is found that the pulsating mode quickly kicks in for the range of inlet velocity conditions chosen. This results in a large fluctuation in flame temperature (around 150 K) and flame consumption speed (around 60 cm/s) as shown in Figure 2.

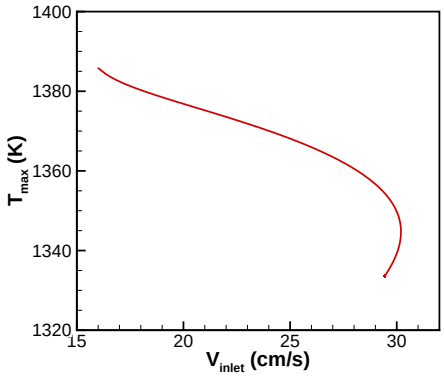

Figure 1: Upper-branch of the inverse S-curve. Steady state value of maximum temperature is plotted against inlet velocity.

It is observed that as the inlet velocity becomes closer to the extinction turning point, the amplitude of the oscillations becomes increasingly larger. For example, for the case with V_{inlet} = 20 cm/s, the flame sustains temperature excursions as low as 1330 K, which is lower than the steady extinction turning point temperature (see Figure 1). For V_{inlet} > 20 cm/s, the flame is unable to sustain pulsations and extinction occurs after a few pulsation cycles. This phenomenon is henceforth referred to as oscillatory extinction. Note that this oscillatory extinction limit is much lower

than that found using steady state simulations. This is consistent with findings from a previous study [3]. For the steady state simulation with V_{inlet} = 20 cm/s, the flame time scale (τ_{flame}) (defined as L/S_L where L is the thermal flame thickness [16], and S_L is the flame consumption speed) is found to be 0.74 ms. This corresponds to the intrinsic flame frequency of 1350 Hz. The average time period of pulsation ($\tau_{pulsation}$) at this condition is found to be 5.6 ms, which corresponds to a pulsation frequency of 178.6 Hz. Thus, the pulsation frequency is found to be much smaller than the intrinsic flame frequency.

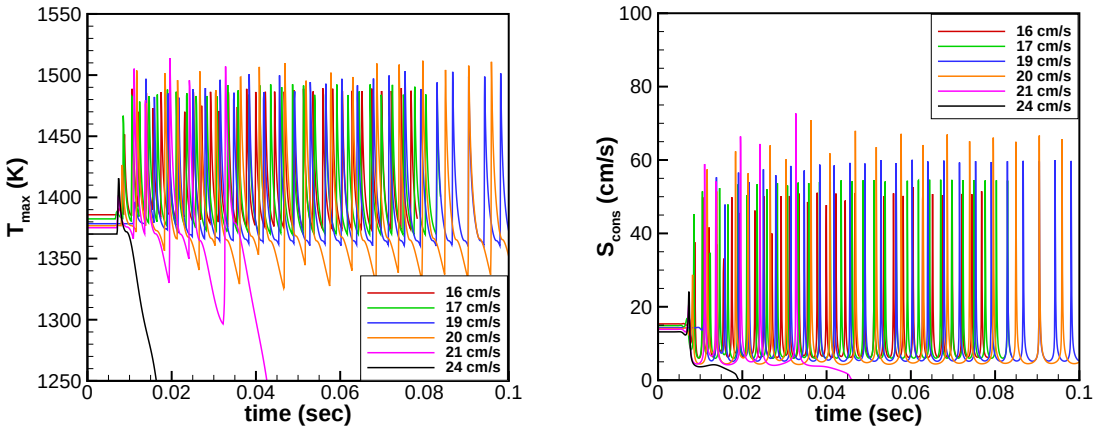

(a) (b)

Figure 2: Evolution of maximum temperature and flame consumption speed in time for various inlet velocities.

Next, we study the effects of imposing an external fluctuation in strain rate onto the pulsating flame. This is done by sinusoidally fluctuating the inlet flow velocity. A range of forcing frequencies (f), ranging from values much less than pulsation frequency to much greater than intrinsic flame frequency, is investigated. The initial nozzle inlet velocity V_0 is fixed to 16 cm/s for all cases, and the amplitude A is fixed to 0.25; therefore, the velocity at the nozzle inlet fluctuates between 16 cm/s and 24 cm/s. Note again that for steady inlet velocity conditions, $V_{inlet} > 20$ cm/s leads to oscillatory extinction.

Figure 3 shows the response of maximum temperature and flame consumption speed in time. Compared to cases with steady inlet velocity, we see that pulsation in unsteady cases appears almost immediately. From the top row of Figure 3 it is seen that if the forcing frequency is less than the pulsation frequency (= 178.6 Hz at V_{inlet} = 20 cm/s), oscillatory extinction occurs. For these frequencies the minimum and maximum values of the flame response also vary with time. For frequencies very close to this pulsation frequency, such as f = 150 Hz, the oscillatory extinction occurs after a very large number of pulsation cycles (in this case it occurs at around 200 ms). From a practical perspective, combustion devices such as internal combustion engines in which the combustion is not continuous in time, a time of 200 ms may be large enough to disregard this oscillatory extinction behavior. For frequencies greater than the pulsation frequency, i.e. f = 200 Hz in the top row figures and all frequencies in the bottom row figures, the flame is able to sustain pulsations indefinitely. This can be deduced from the observation that, after a few pulsation cycles, the minimum and maximum values of the flame temperature oscillation reach a fixed value, unlike for the low frequency cases. Moreover, for these

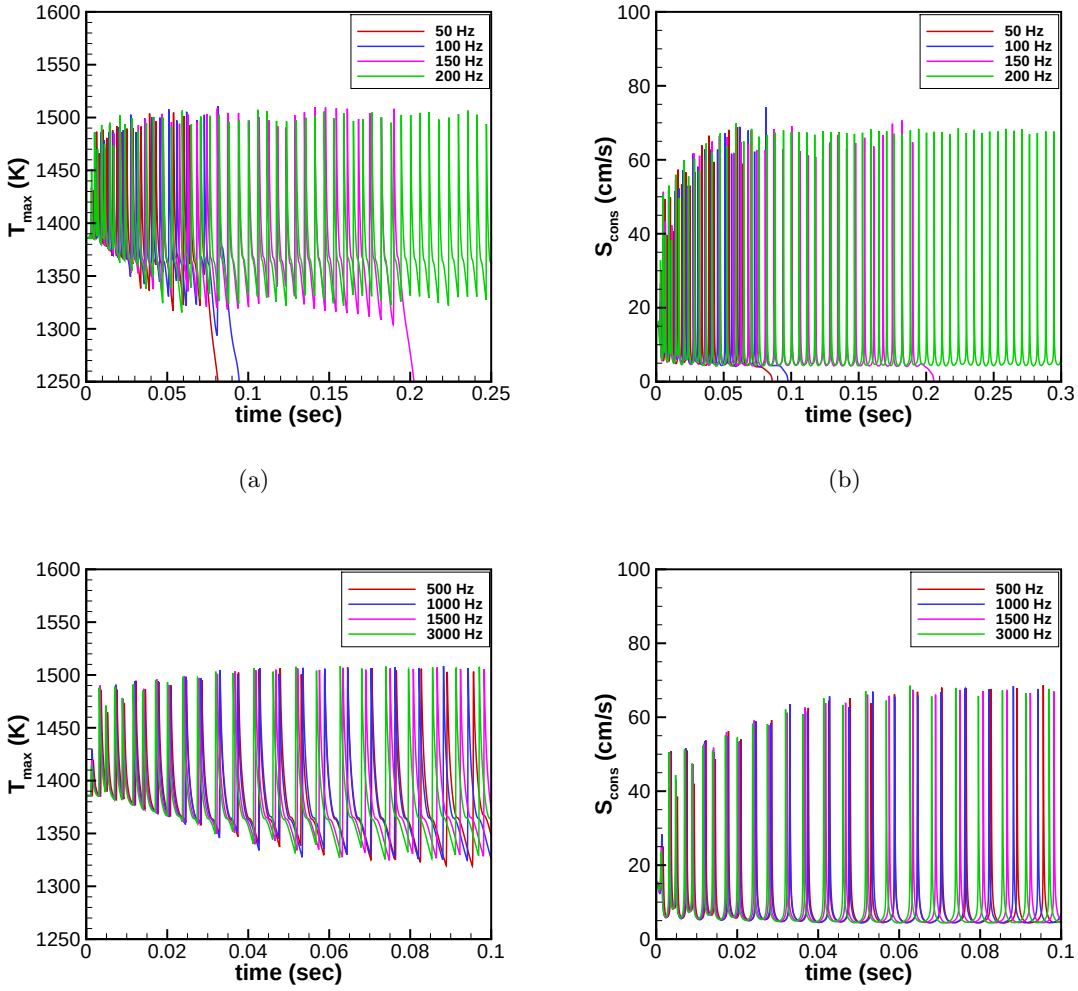

Figure 3: Evolution of maximum temperature and flame consumption speed in time for various forcing frequencies. Top figures: frequencies lower or close to pulsation frequency. Bottom figures: frequencies greater than the pulsation frequency, 178.6 Hz.

high frequencies, the flame is found to be unresponsive to the upstream velocity fluctuations. This can be seen in the bottom row plots in Figure 3, where the flame temperature and consumption speed response is relatively insensitive as the frequency increases from 500 Hz to 3000 Hz. Another interesting feature of these pulsating instabilities is the large modification of the internal flame structure. Figure 4 shows the flow velocity and temperature profiles of the flame at times corresponding to a trough (solid line) and a peak (dashed line) in consumption speed response, for $f = 1500$ Hz case. Note the significant jump in flow velocity as pulsation occurs. The pulsation actually results in positive velocities upstream of the flame. This leads to flow reversal upstream of the flame. Flow reversal is a clear manifestation of the presence of flame strongly affecting the upstream flow field, and is also studied in detail in Ref. [17] in a similar configuration. The temperature profile exhibits a spike of approximately 200 K as pulsation occurs. In the next section we will present results of 2D simulations of these pulsating flames.

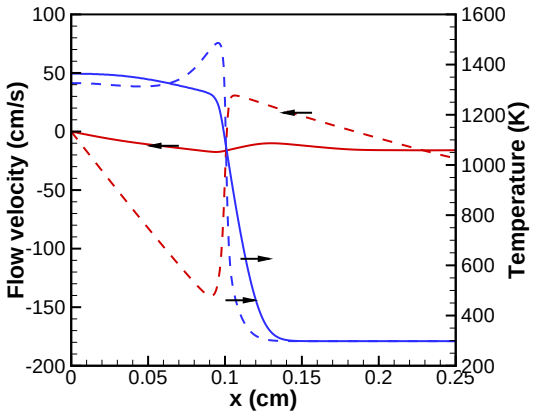

Figure 4: Flow velocity and temperature profiles of the flame at times corresponding to a trough (solid line) and a peak (dashed line) in consumption speed response, for $f = 1500$ Hz case.

4 Two-Dimensional Flame Results

As mentioned in Section 2, the two-dimensional axisymmetric simulations were conducted in a reactant-to-product counterflow configuration. Reactants enter from the right boundary and adiabatic products enter from the left boundary. The velocity inlet boundary conditions were chosen such that the strain rate (maximum axial velocity gradient upstream of the flame) is close to the one-dimensional case with $V_{inlet} = 20$ cm/s. Figure 5 shows the evolution of maximum temperature and maximum OH mass fraction in the domain with time. The pulsating instability appears soon after the start of the simulation. It is also observed that after several pulsations, twin-peaks appear in the flame response. A previous study [3] also reported the occurrence of such a regime of twin-peaks or period-doubling. Figure 6 shows the temperature (top row) and OH mass fraction (bottom row) fields for four different times. Streamlines are overlaid on the temperature field in the upper row figures. Plot (a) shows the fields at a time when the flame is in a weak "hibernating" mode. There is very little divergence of streamlines across the flame as the heat release, and consequently the gas expansion across the flame, is small. A very faint OH profile is observed at this time. Plots (b) and (c) correspond to times at which the flame

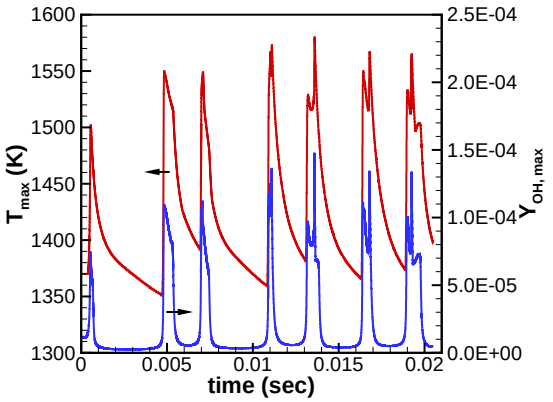

Figure 5: Maximum temperature and maximum OH mass fraction evolution in time.

goes through a pulsation, and a strong surge in temperature and OH mass fraction is observed. It is interesting to note that the flame surface no longer remains flat, but two cells develop on the flame surface, as revealed in plot (b). The cells grow laterally on the flame surface and annihilate each other, and in plot (c) they have merged to form a cusp. The OH mass fraction is high at the convex regions near the center of these cells, and once the cells merge to form a cusp, OH is concentrated at the cusp. There is a strong divergence of streamlines away from the cells in plot (b) and away from the cusp in plot (c). At some locations the divergence is so strong that the flow completely reverses direction upstream of the strongly burning flame element. Plot (d) shows the fields at a later time when the flame goes through another pulsating cycle. It is observed that the location of formation of these cells is random, and sometimes one, and other times two cells emerge as pulsation occurs. It is also observed that the cells do not achieve a steady state or a fixed finite length scale, but quickly disappear as the flame transitions back into the weakly burning "hibernating" mode. The reason for formation of cells on the flame surface may be attributed to the coupled effects of pulsating and hydrodynamic instabilities: Due to the pulsating instability mode local regions of the flame burn much stronger compared to the rest of the flame. This causes a sudden increase in gas expansion across these regions and consequently a strong flow divergence upstream of these strongly burning regions, which inturn grow due to hydrodynamic instability.

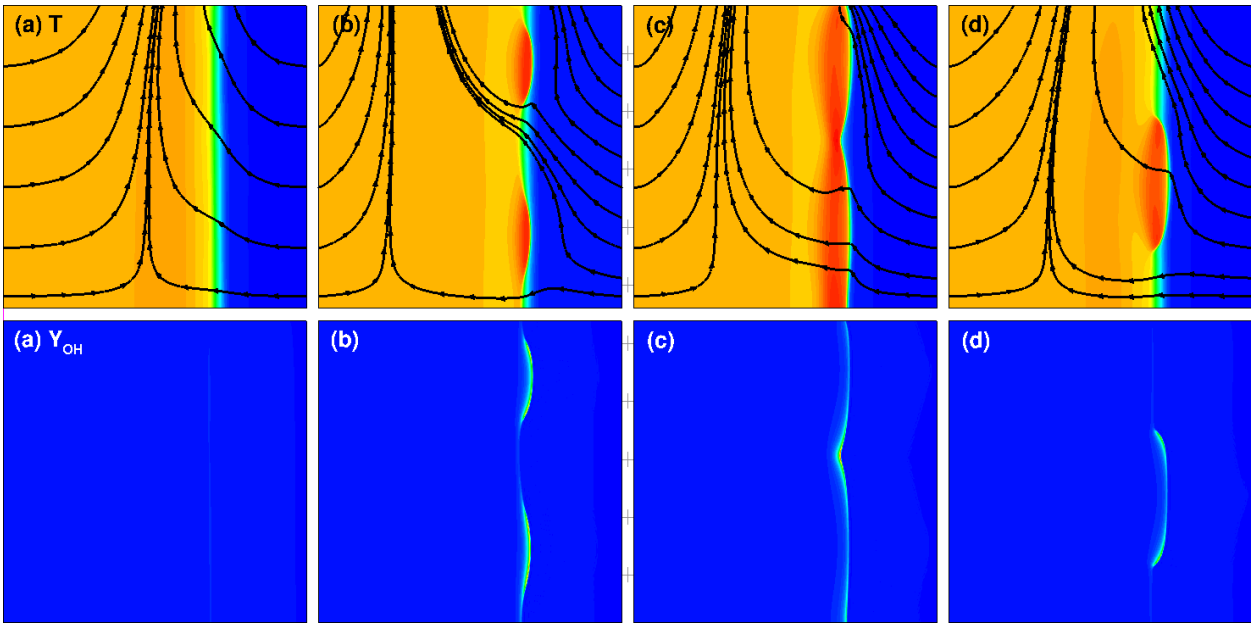

Figure 6: Temperature (top row) and OH mass fraction (bottom row) fields for four different times: (a) 8.95 ms, (b) 10.95 ms, (c) 11.1 ms, (d) 13.3 ms. Streamlines overlaid on temperature field in top row figures. Color scale: For temperature, 298 K (blue) to 1570 K (red), for OH mass fraction, 0 (blue) to 1.18e-4 (red).

5 Concluding Remarks

In this paper, we studied the pulsating instability mode in near-rich limit hydrogen/air premixed flames in a counterflow configuration. One- and two-dimensional simulations were conducted using detailed hydrogen/air chemical kinetics. For one-dimensional flames, an unsteady monochromatic flow field was imposed on the flame by sinusoidally fluctuating the nozzle inlet flow velocity. A

range of values of forcing frequency was investigated varying from values much smaller than the pulsation frequency to those much larger than the intrinsic flame frequency. For the amplitude and mean value of the inlet velocity chosen, the flame was found to undergo oscillatory extinction if the forcing frequency was less than the pulsation frequency. For forcing frequencies higher than the pulsation frequency, the flame was found to be largely unresponsive to the upstream flow velocity fluctuations. The flame structure during pulsation revealed presence of flow reversal upstream of the flame base, thereby indicating that the pulsating flame strongly affects the upstream flow field.

Two-dimensional simulations showed that cell and cusp formation occurs on the flame surface as the flame is subjected to several pulsation cycles. The initiation location of the cells was found to be random, and sometimes one and other times two cells were found to exist. These cells were found to grow laterally on the flame surface, and quickly disappeared as the flame transitioned back into the weakly burning "hibernating" mode. Similar to the one-dimensional case, strong flow divergence and also flow reversal upstream of flame base was found to occur in two-dimensional simulations. In an ongoing study, we are studying the effects of turbulence on pulsating flames, by injecting turbulent-like vortices from the reactant nozzle in the two-dimensional simulations. It is conjectured that because of the strong surge in burning rate of the flame during these pulsations, any wrinkling induced by turbulent straining would relax, similar to the one-dimensional case where the flame was found to be unresponsive to the upstream velocity fluctuations.

Acknowledgments

The work was supported by the Division of Chemical Sciences, Geosciences, and Biosciences, Office of Basic Energy Sciences and the Combustion Energy Frontier Research Center, an Energy Frontier Research Center funded by the U.S. Department of Energy, Office of Science, Office of Basic Energy Sciences under Award Number DE-SC0001198. SNL is a multiprogram laboratory operated by Sandia Corporation, a Lockheed Martin Company, for the US Department of Energy under contract DE-AC04-94AL85000.

References

[1] G. I. Sivashinsky. *Combustion Science and Technology*, 15:137–146, 1977.

[2] C. J. Sung, A. Makino, and C. K. Law. *Combustion and Flame*, 128:422–434, 2002.

[3] E. W. Christiansen, C. K. Law, and C. J. Sung. *Combustion and Flame*, 124:35–49, 2001.

[4] J. Yuan, Y. Ju, and C. K. Law. *Combustion and Flame*, 144:386–397, 2006.

[5] G. Jomaas and C. K. Law. *Physics of Fluids*, 22:124102, 2010.

[6] E. W. Christiansen, C. K. Law, and C. J. Sung. *Proceedings of the Combustion Institute*, 29:61–68, 2002.

[7] H. G. Im, L. L. Raja, R. J. Kee, and L. R. Petzold. *Combustion Science and Technology*, 158:341–363, 2000.

[8] R. J. Kee, F. M. Rupley, and J. A. Miller. Chemkin-II: A fortran chemical kinetics package for the analysis of gas-phase chemical kinetics. Technical Report SAND89-8009B, Sandia National Laboratories, 1991.

[9] R. J. Kee, G. Dixon-Lewis, J. Warnatz, M. E. Coltrin, and J. A. Miller. A fortran computer code package for the evaluation of gas-phase multicomponent transport properties. Technical Report SAND86-8246, Sandia National Laboratories, 1986.

[10] T. Poinsot, T. Echekki, and G. Mungal. *Combustion Science and Technology*, 81:45–73, 1992.

[11] C. A. Kennedy and M. H. Carpenter. *Applied Numerical Mathematics*, 14(4):397–433, 1994.

[12] C. A. Kennedy, M. H. Carpenter, and R. M. Lewis. *Applied Numerical Mathematics*, 35(3):177–219, 2000.

[13] C. S. Yoo and H. G. Im. *Combustion Theory and Modelling*, 11:259–286, 2007.

[14] C. S. Yoo, J. H. Chen, and J. H. Frank. *Combustion and Flame*, 156:140–151, 2009.

[15] J. Li, Z. Zhao, A. Kazakov, and F. Dryer. *International Journal of Chemical Kinetics*, 36:566–575, 2004.

[16] D. B. Spalding. *Some Fundamentals of Combustion*. Butterworths, London, 1955.

[17] G. Bansal, H. G. Im, and J. K. Bechtold. *Combustion and Flame*, (in review).